Detailed mapping and statistical analysis of Noachian and post-Noachian valley networks: implications to the history of martian surface environment. Yumu Yamaguchi[1], Hideaki Miyamoto[1], Kenneth L. Tanaka[2], James M. Dohm[1,3], and Trent M. Hare[3], [1] University of Tokyo, Tokyo 113-0033, Japan, [2] U. S. Geological Survey, Flagstaff, Arizona, USA, [3] Department of Hydrology and Water Resources, University of Arizona, Tucson, USA

Introduction: Most of the Noachian cratered highlands and some of the flanks of post-Noachian volcanoes of Mars are dissected by networks of branching valleys, whose evolutionary history remains controversial [e.g., 1, 2]. The heads of valleys occur at sharp ridge crests, which may indicate that the valleys are cut primarily by surface runoff following precipitation [e.g., 3]. However, stubby tributaries and amphitheater heads of valleys may favor groundwater sapping [4]. Some researchers maintain that the formational mechanisms of valley networks vary according to space and/or time [e.g., 5, 6]. Revealing formational processes of valley networks through space and time (Noachian and post-Noachian) gives us clues to the history of the martian paleoenvironment, especially the circulation of both atmospheric and ground water.

To quantitatively compare characteristics between valley networks in different regions, we identify valley networks precisely as possible, and extract indices of them. Among these indices, we focus on the valley distribution as it may indicate the maturity of the valley systems. We perform statistical analyses of the distributions of the Noachian and post-Noachian valley networks, pointing to their formational processes through space and time.

Mapping Investigation: For our detailed mapping investigation, we use Thermal Emission Imaging System (THEMIS) infrared (IR) daytime images (100 m/pixel), and where there are gaps in THEMIS coverage, the Viking MDIM 2.1 image mosaic (231m/pixel). In addition, the MOLA digital elevation model (about 460 m/pixel) is utilized to both avoid false positives and determine drainage divides and local slopes.

Although automatic identification of valley shapes on MOLA topography data by using computer software is advantageous in mapping a wider area in a shorter time [e.g., 7], small valleys go unnoticed without the use of high-resolution images (automated procedures are difficult to apply to such data). As a complementary approach, we mapped the valley networks manually.

Noachian Valley Networks: Valley network systems of a typical Noachian terrain are mapped, characterized, and their drainage densities tallied in (1) the region around and in Naktong Vallis, and (2) the region around and in Licus Vallis (Figure 1). Because these two regions are sufficiently distant (more than 5,000 km), the climate and/or lithology when forming the valley networks, as well as formational conditions or processes of valley networks, can be distinct.

The region around and in Naktong Vallis consist of 36 major valley systems of Late-Noachian age [8] (Figure 1B). In this region, the total length of the valley networks is more than 66,000 km, and each drainage area ranges from 9,000 to 210,000 km^2. We focus on the drainage density, which is the valley length of each valley network divided by the total drainage area of each system. This quantitative spatial information represents the distribution of valleys.

We find a positive correlation between the drainage densities and the mean slopes of the drainage areas (Figure 2). The systematic increase in the drainage density with the mean slope suggests that the control of slope is significant to the formational processes of the valley networks. Thus, water may have been supplied by precipitation with the mean slope of the precipitated area generally controlling the velocity of the resultant surface runoff. Therefore, we suggest that the most likely source of water for the formation of valley networks in the region around and in Naktong Vallis is precipitation, though groundwater may have also contributed to valley network formation during the precipitation phase.

The region around and in Licus Vallis consist of 7 major valley systems of Late-Noachian age [8] (Figure 1C). In this region, the total length of the valley networks is more than 19,000 km, and each drainage area ranges from 2,300 to 45,000 km^2.

We focus on the relationship between the drainage densities and the mean slopes, and reveal the positive correlation between these indices similar to the valley networks within the region around and in Naktong Vallis (Figure 2). This indicates that the formational processes of the valley networks in both distant regions may have been surface runoff after precipitation.

Interestingly, all the exceptions of this correlation represent the valley networks in large craters (Figure 1B). Thus, it may imply that the valley networks in large craters were formed mainly by processes other than precipitation [1].

Post-Noachian Valley Networks: Fewer Hesperian and Amazonian (post-Noachian) valley networks exist, and such valley networks, in general, do not form clusters [1, 9]. Consequently, we select several post-Noachian valley networks, which occur apart from each other. They occur on Late Noachian-Early Hes-

perian and younger flanks of Ceraunius, Uranius, and Hecates Tholi and Apollinaris and Hadriaca Paterae [e.g., 9-11] (Figure 1D). We measure their drainage densities and mean slopes, as well as compare their results with those of Noachian valley networks.

Our investigation shows that the ranges of the drainage densities and the mean slopes (tangents of slopes) of post-Noachian valley networks are 0.25 to 0.37km/ km^2 and 0.031 to 0.108, respectively.

A correlation between the drainage densities and mean slopes of the Noachian and the post-Noachian valley networks, which dissect the flanks of Apollinaris and Hadriaca Paterae, exists (Figure 2). Thus, part of the post-Noachian valley networks may also indicate surface runoff, and thus, the precipitation may have been local related to geological phenomena such as impacts [12].

On the other hand, the other part of the post-Noachian valley networks does not indicate correlation similar to Noachian valley networks, because the mean slopes are exceedingly high relative to the drainage densities (Figure 2). Thus, the formational process of part of the post-Noachian valley networks may have been different from that of Noachian valley networks. Though the formational process cannot be constrained,

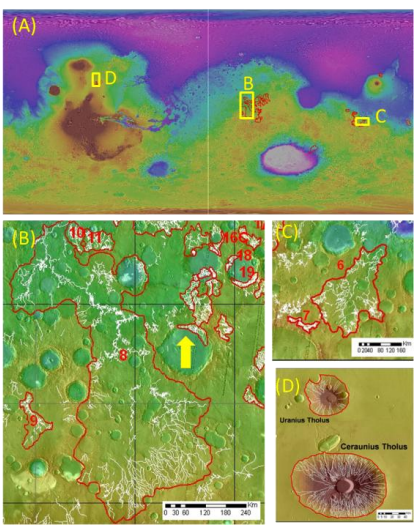

Figure 1. (A) MOLA topographic map of whole Mars showing sites of investigation. Red lines indicate the boundaries of 48 drainage areas, which contain systems of valley networks. (B) Close-up of site B showing part of region around and in Naktong Vallis. White lines represent valleys. Yellow arrow indicates a valley network in a large crater. (C) Close-up of site C showing region around and in Licus Vallis. (B) and (C) include Noachian valley networks. The red-highlighted numbers mark specific drainage areas. (D) Uranius and Ceranius Tholi. The flanks of these volcanoes are dissected by post-Noachian valley networks.

it must have been influenced by processes other than (or in addition to) precipitation, such as the drainage from a caldera lake, which had been formed due to the melting of snow on the summit of the volcano [13].

Our results suggest that the Late-Noachian epoch records a warmer and wetter climate when compared to the post-Noachian Periods, including the possibility of atmospheric water circulation. Though valley formation occurred on the flanks of volcanoes, the process of valley formation appears not to have been the same in each case. Further investigation is necessary to better understand these distinctions in space and time.

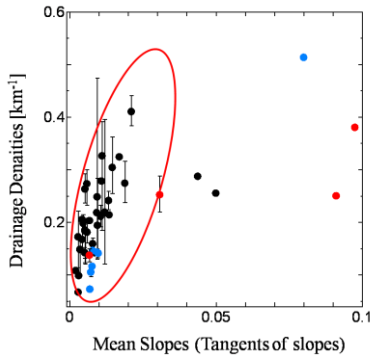

Figure 2. Drainage density vs. mean slope (tangents of slopes) of the drainage areas. Black dots represent drainage areas, which contain Noachian valley networks on the region around and in Naktong Vallis, blue dots Noachian valley networks on the region around and in Licus Vallis, and red dots post-Noachian valley networks.

References: [1] Carr M.H. (2006) The Surface of Mars. [2] Craddock R.A. and Howard A.D. (2002) *JGR*, *107*, E11. [3] Hynek B.M. and Phillips R.J. (2003) *Geology*, *31*, 757-760. [4] Gulick V.C. (2001) *Geomorphology*, *37*, 241-268. [5] Luo W. and Howard A.D. (2005) *JGR*, *110*, E12S13. [6] Harrison K.P. and Grimm R.E. (2005) *JGR*, *110*, E12S16. [7] Luo W. and Stepinski T.F. (2009) *JGR*, *114*, E11010. [8] Fassett C.I. and Head J.W. (2008) *Icarus*, *195*, 61-89. [9] Scott D.H. et al. (1995) USGS Misc. Inv. Ser. Map I-2461. [10] Scott D.H. and Tanaka K.L. (1986) USGS Misc. Inv. Ser. Map I-1802-A. [11] Greeley R. and Guest J.E. (1987) USGS Misc. Inv. Ser. Map I-1802B [12] Segura T.S. et al. (2002) *Science*, *298*, 1977-1980. [13] Fassett C.I. and Head J.W. (2007) *Icarus*, *189*, 118-135.